INFECTION AND IMMUNITY, July 2005, p. 4161–4170 Vol. 73, No. 7
0019-9567/05/$08.00+0 doi:10.1128/IAI.73.7.4161–4170.2005

Superoxide Production in *Galleria mellonella* Hemocytes: Identification of Proteins Homologous to the NADPH Oxidase Complex of Human Neutrophils

David Bergin,[1]† Emer P. Reeves,[1]† Julie Renwick,[1] Frans B. Wientjes,[2] and Kevin Kavanagh[1]*

Medical Mycology Unit, National Institute for Cellular Biotechnology, Department of Biology, NUI Maynooth, Co. Kildare, Ireland,[1] and Centre for Molecular Medicine, University College London, 5 University Street, London WC1E 6JJ, United Kingdom[2]

Received 4 January 2005/Returned for modification 11 February 2005/Accepted 7 March 2005

The insect immune response has a number of structural and functional similarities to the innate immune response of mammals. The objective of the work presented here was to establish the mechanism by which insect hemocytes produce superoxide and to ascertain whether the proteins involved in superoxide production are similar to those involved in the NADPH oxidase-induced superoxide production in human neutrophils. Hemocytes of the greater wax moth (*Galleria mellonella*) were shown to be capable of phagocytosing bacterial and fungal cells. The kinetics of phagocytosis and microbial killing were similar in the insect hemocytes and human neutrophils. Superoxide production and microbial killing by both cell types were inhibited in the presence of the NADPH oxidase inhibitor diphenyleneiodonium chloride. Immunoblotting of *G. mellonella* hemocytes with antibodies raised against human neutrophil *phox* proteins revealed the presence of proteins homologous to gp91^{phox}, p67^{phox}, p47^{phox}, and the GTP-binding protein rac 2. A protein equivalent to p40^{phox} was not detected in insect hemocytes. Immunofluorescence analysis localized insect 47-kDa and 67-kDa proteins throughout the cytosol and in the perinuclear region. Hemocyte 67-kDa and 47-kDa proteins were immunoprecipitated and analyzed by matrix-assisted laser desorption ionization—time of flight analysis. The results revealed that the hemocyte 67-kDa and 47-kDa proteins contained peptides matching those of p67^{phox} and p47^{phox} of human neutrophils. The results presented here indicate that insect hemocytes phagocytose and kill bacterial and fungal cells by a mechanism similar to the mechanism used by human neutrophils via the production of superoxide. We identified proteins homologous to a number of proteins essential for superoxide production in human neutrophils and demonstrated that significant regions of the 67-kDa and 47-kDa insect proteins are identical to regions of the p67^{phox} and p47^{phox} proteins of neutrophils.

Neutrophils play a pivotal role in the innate immune response of mammals by phagocytosing and destroying invading microorganisms (39). Serum-opsonized microbes can be killed within the confines of the phagocytic vacuole, a process which is dependent upon the generation of reactive oxygen species (ROS) (55), predominantly superoxide (O_2^-) and hydrogen peroxide (H_2O_2) (2). In addition to the dismutation products of O_2^-, this anion has also been shown to be indirectly responsible for the activation of cationic granule enzymes, such as elastase and cathepsin G, which then participate in the destruction of the microbes (55).

The NADPH oxidase complex of neutrophils is a highly regulated multicomponent system, and the absence of this system or an abnormality in it results in disease, such as chronic granulomatous disease (CGD) (33), which is characterized by a profound predisposition to infection. The plasma membrane and the membrane of the specific granules of neutrophils contain a flavocytochrome *b* (flavocytochrome b_{558}), which is incorporated into the membrane of the phagocytic vacuole (59). Flavocytochrome *b* is a heterodimer composed of gp91^{phox} and p22^{phox} (phox indicates phagocyte oxidase) at a molar ratio of 1:1 (68). gp91^{phox} contains NADPH and flavin adenine dinucleotide binding sites in its soluble cytosolic domain (61). The activated flavocytochrome b_{558} works as the catalytic redox center, where electrons are transferred from NADPH to molecular oxygen to generate O_2^-. A number of homologues of this protein have been discovered, including Nox1 to Nox5 (10, 45), p138Tox in thyroid (23), renox in the kidney (30), and rbohA in plants (35). p22^{phox} is required for gp91^{phox} stability and appears to bind soluble cytosolic activating factors (64). These factors include p67^{phox}, p47^{phox}, and the small GTP-binding protein rac in the GTP-bound form, which together with amphiphiles such as sodium dodecyl sulfate (SDS) and membranes or pure flavocytochrome induce electron transport in vitro, in what is known as the "cell-free system" (13). Another protein, p40^{phox} (69), also binds strongly to p67^{phox}. p40^{phox} becomes phosphorylated when the NADPH oxidase is activated; however, the role of this *phox* protein is controversial since both stimulatory (66) and inhibitory effects (17) on the oxidase have been observed. These cytosolic proteins interact with each other (28, 29, 70), with rac (19, 20), and with the flavocytochrome (15, 16, 21) through a number of *Src* homology 3 (SH3), proline-rich, tetratricopeptide repeat, and PC motifs (53).

The immune system of insects exhibits a high degree of structural and functional similarity with the innate immune system of mammals (41, 57, 67). The insect hemolymph con-

* Corresponding author. Mailing address: Medical Mycology Unit, NICB, Department of Biology, NUI Maynooth, Co. Kildare, Ireland. Phone: 353-1-7083859. Fax: 353-1-7083845. E-mail: kevin.kavanagh@may.ie.

† D.B. and E.P.R. contributed equally to this work.

tains hemocytes, which function in a manner similar to that of phagocytes of humans (54). At least six types of hemocytes have been identified in insects such as *Galleria mellonella* (the greater wax moth) (7), and plasmatocytes and granulocytes are the most abundant phagocytic cell types. NADPH oxidase and NO synthase pathways have been observed in the self-defense system of *Mytilus galloprovincialis* (1), and production of ROS has also been detected in hemocytes; evidence of both O_2^- (32) and its dismutation product, H_2O_2, has been found in plasmatocytes of *Drosophila melanogaster* larvae (51) and *G. mellonella* (62).

Similarities between vertebrate and invertebrate immune cells extend to the signal transduction pathways that trigger their activation. In phagocytic cells of vertebrates there are two pathways leading to NADPH oxidase activation, and these pathways are Ca^{2+} and protein kinase C (PKC) dependent or independent and are activated by phorbol-12-myristate-13-acetate (PMA) and concanavalin-coated particles, respectively (18, 72). In bivalve mollusks, phorbol esters have been shown to stimulate the hemocyte NADPH oxidase pathway directly at the level of PKC (3), whereas laminarin has been reported to interact with beta-1,3-glucan-binding proteins on the hemocyte surface in arthropods and mollusks and to activate the whole oxidase pathway (63).

The similarities between the oxidative burst pathways of insect hemocytes and mammalian neutrophils raise the possibility that the complexes that generate the ROS might also contain homologous components. Recent reports have provided evidence for the involvement of proteins homologous to human neutrophil $p47^{phox}$ and $p67^{phox}$ (5, 31), which support superoxide generation by the NADPH oxidase NOX and are termed NOXO1 and NOXA1. In addition, both *phox* proteins have been detected immunologically in cultured plant cells and possibly participate in the soybean cell oxidative burst (24). Thus, an examination of whether membrane and cytosolic *phox* proteins are present in insect hemocytes would provide a stringent test of the homology between the insect and mammal oxidase complexes. Most immunological data for insects are data for *D. melanogaster*; however, in *G. mellonella*, various immunorelevant protein molecules have been described, and this system is being increasingly used as a model for assessing the virulence of a range of microorganisms (41). Larvae of *G. mellonella* have been used to evaluate the pathogenicity of lipopolysaccharide-deficient mutants of *Pseudomonas aeruginosa* (22), and there is a good correlation between the virulence of *P. aeruginosa* in *Galleria* larvae and the virulence of *P. aeruginosa* in mice (40). Larvae of *G. mellonella* have been employed to differentiate between pathogenic and nonpathogenic fungi (56) and yeasts (11), and a strong correlation between the virulence of *Candida albicans* mutants in insects and the virulence of *C. albicans* mutants in mice has been established (8).

Given the increased use of insects for evaluating microbial virulence (8, 11, 22, 40, 41, 56) and the need to reduce the number of vertebrates used in such testing (4), it is essential to demonstrate that insects are a valid alternative to the use of mammals (41). In the work presented here we compared the abilities of hemocytes of *G. mellonella* and human neutrophils to engulf and kill bacterial and fungal cells. Using immunological and matrix-assisted laser desorption ionization—time of flight (MALDI-TOF) analyses, we observed the presence of both $p47^{phox}$ and $p67^{phox}$ proteins in insect hemocytes, which may participate in the oxidative burst of these hemocytes. This finding further strengthens the similarities between the oxidative burst pathways in the two cell types and supports the use of *G. mellonella* as an alternative to mammals in in vivo pathogenicity assays.

MATERIALS AND METHODS

Chemicals. All chemicals and reagents were the highest purity and were purchased from Sigma Aldrich Chemical Co. Ltd., Dorset, United Kingdom, unless indicated otherwise.

Microbial strains and culture conditions. *Staphylococcus aureus* (originally isolated from a wound infection in St. James's Hospital, Dublin, Ireland) was cultured in Luria-Bertani (LB) broth (Difco Laboratories, Sparks, Md.) at 37°C and 200 rpm in an orbital incubator. Stocks were maintained on LB agar (2% [wt/vol] agar [Difco Laboratories]). *C. albicans* MEN (a kind gift from D. Kerridge, Cambridge, United Kingdom) was cultured in YEPD broth (2% [wt/vol] glucose, 2% [wt/vol] Bacto peptone [Difco Laboratories], 1% [wt/vol] yeast extract [Oxoid Ltd., Basingstoke, England]) at 30°C and 200 rpm in an orbital shaker. Stocks were maintained on YEPD agar plates (YEPD broth supplemented with 2% [wt/vol] agar).

Preparation of human neutrophils and insect hemocytes. Normal human neutrophils were separated from blood collected in 10-ml heparinized vacuum tubes (BD Vacutainer Systems, Plymouth, United Kingdom) by dextran sedimentation and Ficoll-Hypaque (Axis-Shield PoC AS, Oslo, Norway) centrifugation (58). Residual erythrocytes were removed by hypotonic lysis in water to obtain a suspension containing 95% neutrophils. The cells were resuspended in phosphate-buffered saline (PBS) (pH 7.4) containing 5 mM glucose and used immediately.

Insect hemocytes were harvested from sixth-instar larvae of *G. mellonella* (Mealworm Company, Sheffield, United Kingdom). Larvae were stored in wood shavings in the dark at 15°C, and insects weighing between 0.2 and 0.4 g were selected. Larval hemolymph (three or four larvae gave 1 ml) was bled into 9 ml of insect physiological saline (IPS) (65) containing 10 mM EDTA and 30 mM sodium citrate as anticoagulants. A population consisting of 100% hemocytes was pelleted by centrifugation at $500 \times g$ for 5 min in a Beckman GS-6 centrifuge at room temperature. The cells were washed once in IPS and finally resuspended in PBS containing 5 mM glucose.

In vitro phagocytosis of *C. albicans* by human neutrophils and insect hemocytes. *C. albicans* was opsonized using human blood plasma (55) or cell-free hemolymph diluted 1/10 in IPS (1). Phagocytosis was measured by incubating 1×10^7 neutrophils or 1×10^7 hemocytes with 2×10^6 *C. albicans* cells in a rapidly stirred chamber of a Clark type oxygen electrode at 37°C (60). An aliquot was removed immediately after addition of the yeast cells (time zero) and after 15, 30, 45, or 60 min of incubation. The percentages of viable neutrophils and hemocytes before and after phagocytosis were ascertained by the trypan blue exclusion method, and an approximately 8% reduction in viability was observed over 60 min of incubation for both cell types. Three hundred neutrophils or hemocytes were examined microscopically, and the number of phagocytosing cells was ascertained. The mean ± standard error number of internalized yeast cells per neutrophil or hemocyte was determined.

In vitro killing of *S. aureus* and *C. albicans* in neutrophils and hemocytes. Neutrophils (1×10^7 cells) or hemocytes (1×10^7 cells) were incubated at 37°C in PBS (600 μl) in a rapidly stirred chamber. Serum-opsonized *S. aureus* (1×10^7 cells) or *C. albicans* (2×10^6 cells) was added, and killing was measured as described previously (55) in the presence or absence of diphenyleneiodonium chloride (DPI) (5 μM) (12). The percentages of viable cells before and after PMA stimulation were routinely assessed, and the value was found to decrease by approximately 10 and 2% for neutrophils and hemocytes, respectively. Every 15 min an aliquot (100 μl) was removed from the chamber and placed into chilled LB broth for bacteria or into YEPD broth for yeast cells. The cell suspensions were diluted and plated onto LB agar or YEPD agar plates as appropriate. The results were calculated by determining the means ± standard errors from at least three experiments in which colony counts were determined in triplicate for each sample, and the data were expressed as percentages of the original number at time zero.

Oxygen consumption and cytochrome *c* reduction. Oxygen consumption was measured in a temperature-controlled (37°C) chamber that was attached to an oxygen electrode to which sodium dithionate was added for calibration, assuming

that the normal oxygen content of water is 230 nmol/ml (60). An aliquot of cells (10^6 to 10^7 cells in 1 ml) was placed in the chamber and allowed to reach a steady state of respiration. Cells were stimulated with PMA (1 μg/ml) in the presence or absence of DPI (5 μM).

Production of superoxide by 2×10^6 hemocytes after stimulation with PMA (1 μg/ml) was measured by determining the superoxide dismutase (SOD) (50 μg/ml)-inhibitable reduction of cytochrome *c* (2). Absorbance at 550 nm was recorded with a Beckman DU640 spectrophotometer over 30 min.

Electrophoresis and immunoblotting. Samples were run on SDS-polyacrylamide gel electrophoresis (PAGE) minigels (8 to 12.5% polyacrylamide), and protein profiles were visualized by Coomassie blue staining. For Western blotting, the protein was transferred to a nitrocellulose membrane using a semidry blotter for 1 h at 1.4 mA/cm^2. Rabbit and goat polyclonal antisera raised against human p40^{phox}, p47^{phox}, and p67^{phox} (69) were used at a dilution of 1/1,000 for 1 h. Antibodies to gp91^{phox}, PKC δ (Santa Cruz Biotechnology, Inc., Santa Cruz, Calif.), and rac 2 were used at a dilution of 1/1,000 and incubated for 16 h at 4°C. The antibodies to rac 2 were specific and did not cross-react with rac 1 (Santa Cruz Biotechnology). Horseradish peroxidase-conjugated donkey anti-rabbit immunoglobulin G (IgG) (1/5,000 dilution; Amersham Biosciences UK Ltd., Buckinghamshire, England) or rabbit anti-goat IgG (Calbiochem, Merck Biosciences Ltd., Nottingham, United Kingdom) was used to detect reactive bands with the enhanced chemiluminescence system (Pierce Biotechnology, Inc., Rockford, Ill.).

Fractionation and immunoprecipitation of hemocytes and neutrophils. Diisopropyl fluorophosphate (1 mM) was added to pelleted hemocytes and neutrophils (1×10^8 cells) and incubated on ice for 10 min. The cells were resuspended in 200 μl of break buffer [10 mM KCl, 3 mM NaCl, 4 mM $MgCl_2$, 10 mM piperazine-*N*,*N*′-bis(2-ethanesulfonic acid) (PIPES); pH 7.2] (55) containing protease inhibitors (10 μg/ml leupeptin, pepstatin A, aprotinin, and *N*-α-*p*-tosyl-L-lysine chloromethylketone hydrochloride [TLCK]), sonicated (Bandelin Sonopuls; Bandelin Electronics, Germany) three times for 5 s, and centrifuged at 200 × *g* for 10 min at 4°C. The postnuclear supernatant (PNS) was layered on top of a discontinuous sucrose gradient (17% and 34% [wt/wt] sucrose) and centrifuged at 50,000 × *g* for 10 min at 4°C. The cytosolic fraction was removed from above the 17% (wt/wt) sucrose layer, and membranes were recovered from the top of the 34% (wt/wt) sucrose layer. Proteins in these different fractions were separated by SDS-PAGE and Western blotted.

For immunoprecipitation, prechilled 2× solubilization buffer (2% [vol/vol] Triton X-100, 300 mM NaCl, 2% [wt/vol] sodium deoxycholate, and 0.2% [wt/vol] SDS in break buffer with protease inhibitors [10 μg/ml leupeptin, pepstatin A, aprotinin, and TLCK]) was added to the PNS of 2×10^8 cells at a ratio of 1:1. Primary antibody raised against the relevant proteins was added for 1 h on ice, and this was followed by incubation with reconstituted protein A-Sepharose beads overnight at 4°C. The protein A-Sepharose was washed three times in prechilled 1× solubilization buffer containing protease inhibitors and then boiled for 3 min in a minimum volume of 2× Laemmli sample buffer (44). Immunoprecipitates were subjected to SDS-PAGE and stained with Coomassie blue to visualize proteins intended for MALDI-TOF mass spectrometric (MS) analysis.

Immunofluorescence microscopy. Immunofluorescence microscopy was performed as described previously (34). In brief, hemocytes were collected from *Galleria* larvae in IPS and allowed to adhere to methanol-cleaned glass coverslips. The cells were fixed with 4% paraformaldehyde for 10 min and washed in PBS. Then the cells were permeabilized with 0.2% (vol/vol) Triton X-100 in PBS for 10 min, washed in PBS, and blocked with 10 mM $NaBH_4$ for 1 h. After washing with PBS, the cells were incubated with primary antibody against human p47^{phox} or p67^{phox} overnight at 4°C. The slides were washed in PBS and incubated with fluorescein goat anti-rabbit IgG secondary antibody (Stratech Scientific Ltd., Cambridgshire, England) for 1 h. The controls for this experiment included cells alone and cells exposed only to secondary antibody.

MALDI-TOF mass spectrometry. Mass spectrometry of trypsin-digested proteins was performed using an Ettan MALDI-TOF spectrometer (Amersham Biosciences, Freiburg, Germany). All 1.5-ml tubes were siliconized with Sigmacote, and all reagents were high-performance liquid chromatography grade. For peptide analysis, Coomassie blue-stained protein bands were excised from an SDS-PAGE gel and diced finely, before they were incubated with a minimum volume of acetonitrile (Romil Ltd., Cambridge, United Kingdom) for 5 to 10 min. The acetonitrile was replaced with 100 mM NH_4HCO_3, and the preparation was incubated for 5 min, after which an equal volume of acetonitrile–100 mM NH_4HCO_3 (1:1) was added for 15 min. The gel fragments were dried in a vacuum centrifuge (Heto-Holten, Jouan Nordic A/S). Dithiothreitol (10 mM) in 100 mM NH_4HCO_3 (100 μl) was added, and each sample was incubated for 1 h at 37°C, after which the supernatant was removed and the gel pieces were washed twice (10 min each) with 75 μl of 100 mM NH_4HCO_3; the final supernatant was discarded. Iodoacetamide (50 mM) in 100 mM NH_4HCO_3 (100 μl) was added and incubated at 37°C for 20 min in the dark, before the preparation was washed once with 100 mM NH_4HCO_3 and once with acetonitrile–100 mM NH_4HCO_3 (1:1). Gel pieces were dried for 30 min in a vacuum centrifuge. Sufficient digestion buffer (1 μg trypsin, 20 μl 50 mM NH_4HCO_3, 5 mM $CaCl_2$) was added to cover the gel pieces, which were incubated overnight at 37°C. Samples were centrifuged at 12,000 × *g* for 10 min, and the supernatant was removed. Residual peptides were extracted from the gel pieces by adding 50 μl extraction buffer (1% [vol/vol] trifluoroacteic acid, 60% [vol/vol] acetonitrile) and incubating the preparation for 30 min at 37°C before centrifugation and removal of the supernatant. All supernatants were combined, and the preparation was concentrated to 50 μl in a vacuum centrifuge. Samples were mixed at a 1:1 ratio with a saturated solution of α-cyano-4-α-cyano-4-hydroxycinnaminic acid in 0.25% (vol/vol) trifluoroacteic acid–50% (vol/vol) acetonitrile, and 0.3 to 0.5 μl was applied to a MALDI target slide for MALDI-TOF MS analysis. The sequence for neutrophil p47^{phox} and p67^{phox} was obtained from the National Center for Biotechnology Information website (http://www.ncbi.nlm.nih.gov), and the theoretical peptide masses were determined by using MS Digest (http://prospector.ucsf.edu/ucsfhtml4.0/msdigest.htm).

Statistical analysis. Statistical comparisons were made with Student's *t* test using the Sigma Stat statistical analysis package, version 1.00 (SPSS Inc., Chicago, Ill.). A *P* value of <0.05 was considered significant.

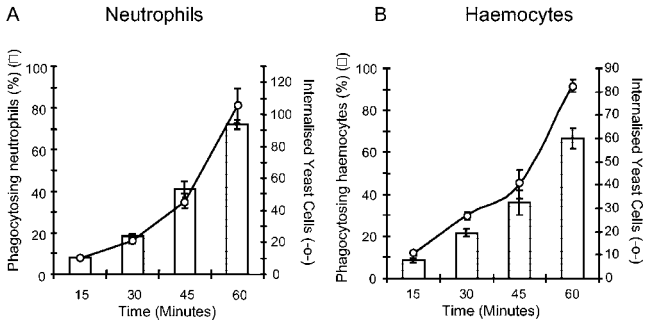

FIG. 1. Kinetics of phagocytosis by neutrophils and hemocytes: in vitro phagocytosis of serum- or hemolymph-opsonized *C. albicans* (2×10^6 cells) by neutrophils (1×10^7 cells) (A) and hemocytes (1×10^7 cells) (B). The scale on the right *y* axis indicates the number of internalized yeast cells per 100 phagocytic cells. Over 60 min, the number of phagocytosing neutrophils (bars) or internalized *Candida* cells (○) was not significantly different from the number of hemocytes (bars) ($P = 0.374$ and $P = 0.26$). Similar results were obtained in two independent experiments. The data are means ± standard errors for three determinations.

RESULTS

In vitro phagocytosis by human neutrophils or insect hemocytes. Phagocytosis and internalization of microbes by neutrophils involve the formation of filopodia that contract and surround and engulf the microorganism. The rates of phagocytosis of *C. albicans* by human neutrophils and insect hemocytes were compared (Fig. 1). Neutrophils internalized serum-opsonized *C. albicans* in vitro, and 18% ± 0.88% of the neutrophils had phagocytosed cells after 30 min of incubation. After 1 h, 72% ± 2.3% of the neutrophils were observed to have phagocytosed cells. The mean number of *Candida* cells internalized per neutrophil remained constant over time (1.25 *Candida* cells per neutrophil) at a *Candida* cell/neutrophil ratio of 1:5. Hemocytes phagocytosed hemolymph-opsonized *C. albicans*, and 21.6% ± 2.0% of the hemocytes had phagocytosed cells after 30 min and 66.85% ± 2.8% of the hemocytes had phagocytosed cells after 60 min. No significant differences in the rates of internalization were observed between neutrophils and hemocytes ($P = 0.26$), and the mean number of *Candida* cells

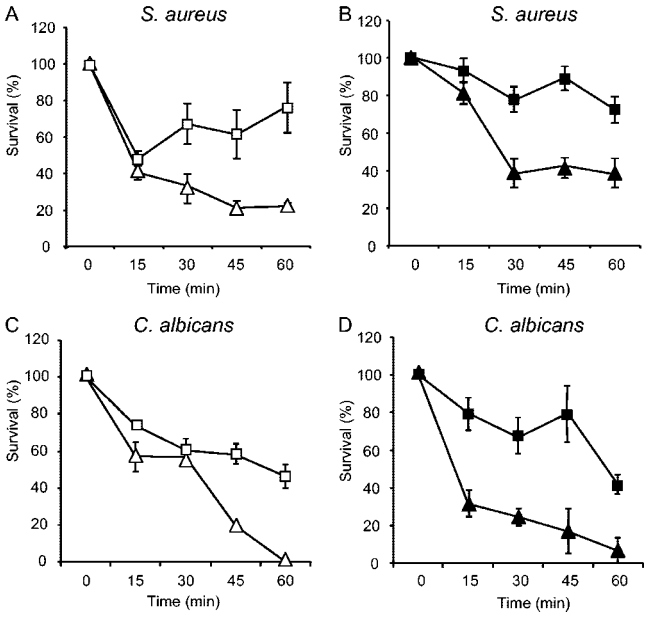

FIG. 2. Kinetics of bacterial and fungal killing by human neutrophils and insect hemocytes. Serum- or hemolymph-opsonized *S. aureus* cells (1×10^7 cells) (A and B) or *C. albicans* cells (2×10^6 cells) (C and D) were exposed to 1×10^7 neutrophils (A and C) or hemocytes of *G. mellonella* (B and D). Killing was also measured in the presence (□ and ■) and in the absence (△ and ▲) of DPI (5 μM) added 3 min prior to initiation of phagocytosis. Microbial survival is expressed as a percentage of the control at time zero, and the data are means ± standard errors. The data are from a representative experiment performed in triplicate.

internalized by hemocytes remained constant (1.18 *Candida* cells per hemocyte) at a hemocyte/*Candida* cell ratio of 1:1.

In vitro killing assays. In order to determine whether human neutrophils and insect phagocytes kill internalized microbes in similar ways, the microbicidal activities of purified neutrophils and hemocytes were determined in vitro. The kinetics of bacterial and fungal killing are shown in Fig. 2 for a ratio of neutrophils or hemocytes to bacterial cells of 1:1 or for a ratio of neutrophils or hemocytes to yeast cells of 5:1. Killing of *S. aureus* by neutrophils occurred quickly, and over 60% ± 3.9% of the bacteria were killed after 15 min (Fig. 2A), as previously described (55). Bacterial killing by hemocytes occurred more slowly; 19% ± 5.5% of the bacteria were killed after 15 min, and 38.3% ± 3.5% of the bacteria were still alive after 30 min (Fig. 2B). Interestingly, there was a difference in the patterns of killing of *S. aureus* and *C. albicans*. At 15 min hemocytes killed *C. albicans* well and *S. aureus* weakly, while the opposite was observed for neutrophils (Fig. 2C and D). After 15 min of incubation hemocytes had killed 68.7% ± 7.0% of the yeast cells, and only 6.6% of the cells remained viable after 60 min. Killing *of C. albicans* by neutrophils was slower, and less than 50% of the cells were killed after 30 min.

The addition of DPI (an inhibitor of NADPH oxidase [12]) greatly impaired the abilities of both neutrophils and hemocytes to kill *S. aureus* and *C. albicans*. Killing of *S. aureus* by neutrophils and hemocytes was reduced by 54% ($P = 0.001$) and 34% ($P < 0.001$), respectively, and killing of *C. albicans* by neutrophils and hemocytes was reduced by 46% ($P = 0.002$) and 35% ($P = 0.013$), respectively, at 60 min compared to the control. These observations confirm the finding that oxidase activity is required by both neutrophils and hemocytes to destroy bacteria (Fig. 2A and B) and yeast cells (Fig. 2C and D). However, the observation that killing by cells treated with DPI was impaired rather than totally inhibited confirms the conclusion that both oxidase activity and nonoxidative granule protease action are necessary for generation of sufficient microbicidal activity to control yeast and staphylococcal infections in vitro (55).

DPI inhibits oxygen consumption and cytochrome *c* reduction by insect hemocytes. Since DPI has been used to document similarity between the oxidative burst complexes of neutrophils and other cell types (1), the effect on oxygen consumption and superoxide production by insect hemocytes was examined. The characteristics of the burst of oxygen consumption by neutrophils and hemocytes after addition of PMA (1 μg/ml) are summarized in Fig. 3. After addition of PMA to neutrophils (1×10^7 cells/ml), there was a lag of about 60 s before oxygen consumption commenced, after which it rapidly increased until it reached a linear rate after about 120 s. The lag in oxygen consumption increased to about 150 s for hemocytes (1×10^7 cells/ml) or neutrophils (1×10^6 cells/ml), and 70 μM oxygen was consumed after 600 s. Oxygen consumption by both cell types was inhibited in the presence of DPI (5 μM) when it was added 3 min prior to the stimulus.

The basis of the proposal that stimulated neutrophils generate O_2^- is the observation that these cells reduce cytochrome *c* in solution and that this reduction is inhibited by SOD (2). Incubation of hemocytes with cytochrome *c* and PMA was found to lead to reduction of the cytochrome, and the O_2^- production was 0.25 ± 0.03 μM/min/10^6 hemocytes (Fig. 4). The O_2^- production was reduced to nearly control values when 5 μM DPI or 50 μg/ml SOD was added to the hemocyte suspension. These decreases in O_2^- generation were statistically significant (for DPI, $P = 0.003$; for SOD, $P = 0.005$) compared to the O_2^- generation of PMA-activated cells.

Western blot analysis of insect hemocyte NADPH oxidase proteins. Immunoblot analysis was performed to characterize

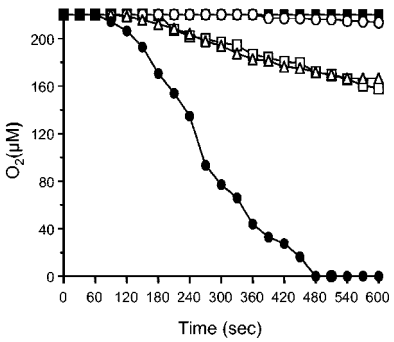

FIG. 3. Inhibition of the hemocyte oxidative burst by DPI. The rate of oxygen consumption by neutrophils (1×10^7 cells [●] or 1×10^6 cells [△]) was compared to the rate of oxygen consumption by insect hemocytes (1×10^7 cells) (□) after stimulation with PMA (1 μg/ml). Oxygen consumption by neutrophils (1×10^6 cells) (○) and hemocytes (1×10^7 cells) (■) was also measured in the presence of DPI (5 μM) added 3 min prior to elicitation. The data are means of three trials carried out on separate days.

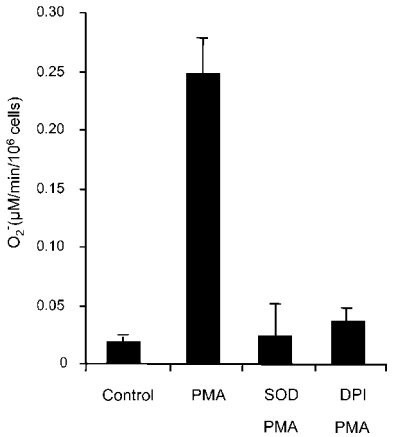

FIG. 4. Effect of an NADPH oxidase inhibitor on in vitro PMA-stimulated generation of O_2^- in hemocytes of *G. mellonella*. The production of O_2^- by unstimulated hemocytes (1×10^6 cells/ml) (Control) and PMA (1 μg/ml)-activated cells was measured using the reduced cytochrome *c* assay. Production of O_2^- by hemocytes was inhibited in the presence of DPI (5 μM) and scavenged in the presence of SOD (50 μg/ml).

the components of the insect hemocyte NADPH oxidase system. Human neutrophil membranes and cytosol fractions (Fig. 5A) were employed. Hemocyte membranes were not observed on the conventional 17% and 34% (wt/wt) sucrose gradient, and therefore, total hemocyte PNS, containing a mixture of cellular membranes and cytosol, was employed. By Western blotting, rabbit polyclonal antibodies against human $p40^{phox}$, $p47^{phox}$, $p67^{phox}$ (69), and $gp91^{phox}$ proteins were used to identify the relevant proteins in hemocyte lysate. In the neutrophil fraction, $gp91^{phox}$ migrated on SDS-PAGE gels as a broad band, an electrophoretic property characteristic of glycoprotein (38), at an apparent molecular mass of 90 kDa (Fig. 5B). Using antibodies to human $gp91^{phox}$, an immunoreactive band was detected in the insect hemocyte PNS at a molecular mass of about 77 kDa, possibly suggesting that this antibody recognizes a region of $gp91^{phox}$ that has remained constant, although the mass of the protein in humans and the mass of the protein in insects are different.

On Western blots for the essential cytosolic components of the NADPH oxidase, $p67^{phox}$ and $p47^{phox}$ stained a single band in samples of human neutrophil cytosol, which migrated like immunoreactive bands in insect hemocyte PNS (Fig. 5C and D). These results indicate that immunologically related proteins having the same molecular masses as $p47^{phox}$ and $p67^{phox}$ are present in insect phagocytic cells. Only one of the *phox* proteins, $p40^{phox}$, was not detected in the insect hemocytes (Fig. 5E).

Another cytosolic component which is required to complement $p47^{phox}$ and $p67^{phox}$ and membranes in the cell-free assay is the small GTP-binding protein rac. rac 2 is expressed predominantly in myeloid cells and is the physiologically active molecule in neutrophils (42). Using polyclonal antibodies specific to rac 2, a single band (Fig. 5F) was detected within neutrophil cytosol and insect hemocyte PNS, again indicating the presence of an immunologically related protein.

Activation of the NADPH oxidase is associated with phosphorylation of $p47^{phox}$, $p67^{phox}$, and $p40^{phox}$. A number of kinases have been implicated in the activation of the oxidase, including PKC (14, 25). Using rabbit polyclonal antibodies to PKC δ, we successfully identified this kinase in cytosol of human neutrophils and PNS of insect hemocytes as an immunoreactive band at 80 kDa (Fig. 5G).

To further strengthen the evidence that O_2^- production in insect phagocytes is associated with proteins which are homologous to components of the NADPH oxidase complex of human neutrophils, fluorescence microscopy was used to determine the distribution of $p47^{phox}$ and $p67^{phox}$ in hemocytes. Cells that had attached to a glass coverslip and spread were ex-

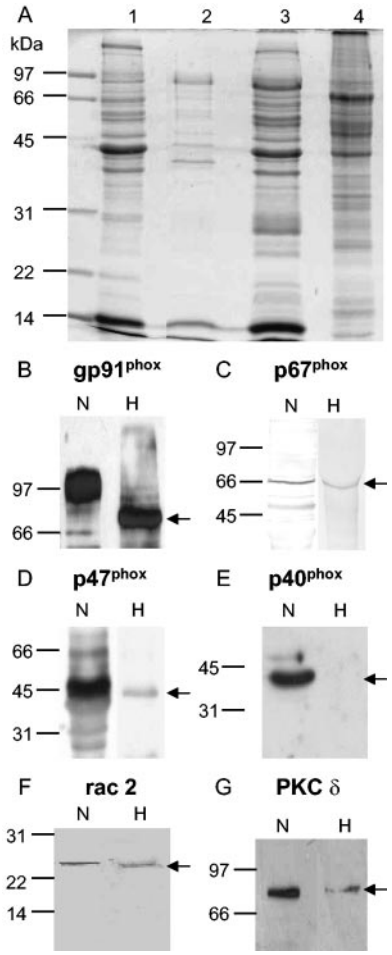

FIG. 5. Immunoblotting of hemocytes of *G. mellonella* with antibodies to human neutrophil *phox* proteins. (A) Coomassie blue-stained SDS-PAGE gel (12.5% polyacrylamide) of neutrophil cytosol (lane 1) and membranes (lane 2). The protein profile of neutrophil PNS (lane 3) was compared to the protein profile of PNS of insect hemocytes (lane 4). The positions of molecular weight markers are indicated on the left. (B) Electrophoretically separated neutrophil membrane proteins and insect hemocyte PNS transferred to nitrocellulose and probed with rabbit antiserum to $gp91^{phox}$. The results show that there was an immunoreactive band at 90 kDa for neutrophil membranes and a band at 77 kDa for insect hemocyte PNS. (C to G) Neutrophil cytosol and insect hemocyte PNS probed with rabbit antisera to $p67^{phox}$ (C), $p47^{phox}$ (D), $p40^{phox}$ (E), rac 2 (F), and PKC δ (G). The results revealed immunologically related proteins having the same molecular mass for all probed proteins except $p40^{phox}$, which was not detected in insect hemocytes.

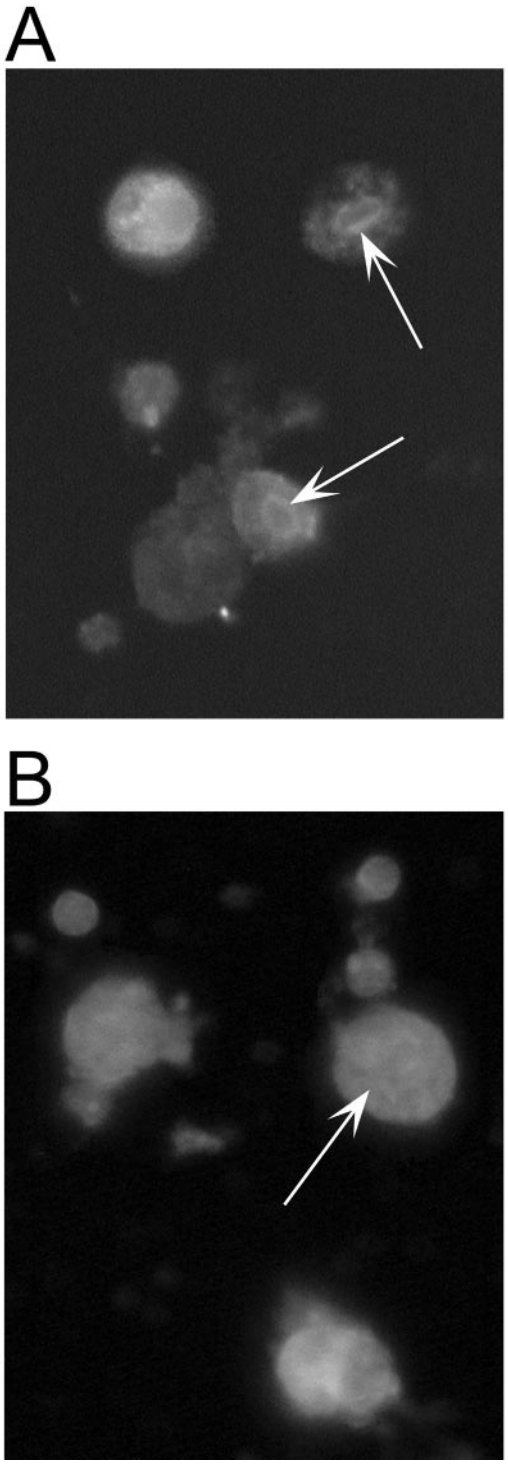

FIG. 6. Distribution of $p47^{phox}$ and $p67^{phox}$ homologues in unstimulated hemocytes: distribution of 47-kDa (A) and 67-kDa (B) insect proteins in hemocytes adhering to glass slides. The distribution of the proteins was predominantly perinuclear (indicated by an arrow) and throughout the cytosol. (magnification, ×400).

amined. The *phox* proteins were located predominantly throughout the cytosol of the cell and in the perinuclear region (Fig. 6). A similar distribution of $p47^{phox}$ and $p67^{phox}$ in unstimulated neutrophils has been described previously (34).

Immunoprecipitation of $p47^{phox}$ and $p67^{phox}$ from hemocytes and neutrophils. To determine the identities of the immunoreactive bands identified by Western blotting, immunoprecipitation was performed using rabbit polyclonal antibodies to $p67^{phox}$ and $p47^{phox}$. Coomassie blue-stained gels are shown in Fig. 7A, in which insect proteins having molecular masses equivalent to those of $p47^{phox}$ and $p67^{phox}$ are visible. Proteins were transferred to a nitrocellulose membrane and probed with goat polyclonal antibodies to the relevant proteins. Figure 7B shows that both neutrophils and hemocytes gave positive signals with goat antibodies raised against $p47^{phox}$ and $p67^{phox}$. Protein bands from the immunoprecipitation were cut from the gel and analyzed by MALDI-TOF MS.

MALDI-TOF analysis of insect proteins. The immunoprecipitated bands that were cross-reactive with the relevant antibodies for human neutrophil $p47^{phox}$ and $p67^{phox}$ were excised from the Coomassie blue-stained gels and digested with trypsin for MALDI-TOF analysis. In the MALDI-TOF spectrum, peptides were observed that had monoisotopic (*m*/*z* tolerance, <1 Da) values very similar to those of a theoretical digest of $p47^{phox}$ and $p67^{phox}$ of human neutrophils.

In the tryptic digest of the insect protein band that was immunoreactive with antibodies to $p67^{phox}$, 10 of 206 peptides (5%) were identified that were similar to peptides of $p67^{phox}$ of human neutrophils (Fig. 8A). This resulted in total protein coverage of 26%. Four of these peptides were located in the conserved domains of $p67^{phox}$, two peptides were located in the first SH3 domain, and two other peptides were located in PB1

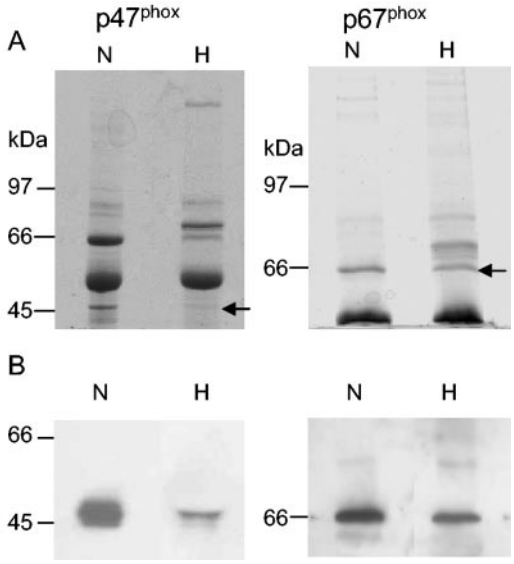

FIG. 7. Immunoprecipitation of $p67^{phox}$ and $p47^{phox}$ from human neutrophils and hemocytes of *G. mellonella*. Postnuclear supernatants were prepared from 2×10^8 neutrophils or hemocytes and solubilized in buffer as described in the text. (A) Immunoprecipitation was carried out using rabbit polyclonal sera against $p67^{phox}$ and $p47^{phox}$, the preparation was resuspended in 60 μl of Laemmli sample buffer, and 25 μl was analyzed by SDS-PAGE and Coomassie blue staining. The positions of immunoprecipitated $p67^{phox}$ and $p47^{phox}$ from neutrophils (N) and hemocytes (H) are indicated by the arrows. (B) Immunoprecipitation preparations were Western blotted using goat polyclonal sera against $p67^{phox}$ and $p47^{phox}$. In two other experiments similar immunoprecipitation results were obtained.

A

p67^{phox}	*M/Z* Observed	Start-end amino acid	Amino acid Sequence	Conserved Domain
	882.371	239-246	ALEGEAHR	SH3 domain 1
	923.918	162-168	AMECVWK	
	950.873	103-110	GNQLIDYK	
	1165.282	346-355	LSVPMPYTLK	
	1505.699	343-355	EVKLSVPMPYLTK	
	1563.623	398-411	DSNELVPLSEDSMK	PB1 domain
	1626.337	233-246	TPEIFRALEGEAHR	
	1731.744	257-271	EELQVMPGNIVFVLK	SH3 domain1
	2048.852	343-359	EVKLSVPMPYTLKVHYK	
	3455.100	459-489	GSQVEALFSYEATQPEDLEFQEGDIILVLSK	SH3 domain 2

B

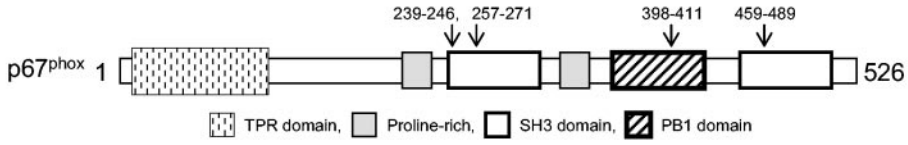

C

p47^{phox}	*M/Z* Observed	Start-end amino acid	Amino acid Sequence	Conserved Domain
	842.416	120-126	VRPDDLK	
	855.026	1-7	MGDTFIR	PX Domain
	868.266	378-384	CSESTKR	
	1076.044	283-292	SGQDVSQAQR	
	1165.245	318-326	RLSQDAYRR	
	1562.662	302-314	RSSIRNAHSIHQR	
	1334.504	307-317	NAHSIHQRSRK	

D

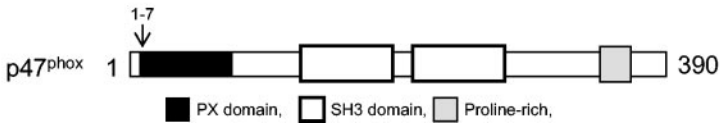

FIG. 8. Matching peptides of hemocyte 67-kDa and 47-kDa proteins to human neutrophil *phox* proteins. (A) Matching peptides of hemocyte 67-kDa protein to human p67^{phox} that strongly reacted with both rabbit and goat anti-human p67^{phox} in immunoprecipitation. (B) Regions of p67^{phox} involved in protein-protein interactions with matching peptides of hemocyte 67-kDa proteins (indicated by arrows). (C) Matching peptides of hemocyte 47-kDa protein to human p47^{phox} that strongly reacted with both rabbit and goat anti-human p47^{phox}. (D) Regions of p47^{phox} involved in protein-protein interactions. Matching peptides of hemocyte 47-kDa protein to neutrophil p47^{phox} in the PX domain is indicated by an arrow.

and the second SH3 domain (Fig. 8B). Seven of 152 peptides were obtained from the tryptic digest of the insect protein immunoreactive with antibodies to p47^{phox}, yielding 16% protein coverage (Fig. 8C). One of the peptides identified was found to lie at the start of the highly conserved PX domain of p47^{phox} (Fig. 8D).

DISCUSSION

Insects are a very successful group of animals and have colonized almost all habitats on the planet except the seas. Their ability to colonize such a diverse range of environments can be explained partially by their efficient immune response. There is a strong structural and functional similarity between the insect immune system and the innate immune system of mammals (41, 57, 67). This has been exploited in recent years by employing insects for assessing the virulence of a range of pathogenic bacteria and fungi. Larvae of *G. mellonella* have been used for evaluating the virulence of mutants of *P. aeruginosa* (22) and for differentiating between pathogenic and nonpathogenic yeast species (11). A strong correlation has been established between the virulence of bacteria (40) and mutants of *C. albicans* in *G. mellonella* and the virulence of these organisms in mice (8). Since the immune response of insects is similar to the innate immune response of mammals, insects have been recognized as valid alternatives for in vivo testing of microbial mutants and may be useful for assessing the efficacy of new antifungal and antibacterial drugs (36).

Phagocytosis requires sequential signal transduction events, and the receptors on the surface of hemolytic plasmatocytes and granulocytes are similar to receptors on mammalian phagocytes (67). Immunity-related proteins and mechanisms that are similar in insects and mammals have been identified,

and the similarities include the remarkable structural and functional similarities between the systems mediating *Drosophila* Toll and mammalian interleukin-1 receptor-mediated signaling (47). A further area of defense where direct comparisons can be drawn is in the synthesis of a broad range of antimicrobial peptides which play a crucial role in combating infection, and similar classes of proteins have been found in vertebrates and invertebrates (67).

The proposed toxic products of NADPH oxidase in neutrophils include superoxide, which quickly dismutates to form hydrogen peroxide. The peroxide and superoxide can react to produce hydroxyl radicals in the presence of metal ions, and hydrogen peroxide can also serve as a substrate for myeloperoxidase-mediated oxidation of halides (37). There has been an accumulation of evidence that ROS are produced in the hemolymph and hemocytes of many insects. The in vitro generation of ROS by hemocytes was studied by electron spin resonance spectroscopy (62) and nitroblue tetrazolium reduction (32). The ROS detected to date include nitric oxide, superoxide, and hydrogen peroxide, and the latter two ROS are required for the production of the highly reactive hydroxyl radical either through the Haber-Weiss reaction or Fenton's reaction (37). In this study the production of ROS by hemocytes was further clarified and extended to include the quantification of oxygen consumption and superoxide production by activated hemocytes. Incubation of the hemocytes with PMA (1 μg/ml) for 10 min resulted in a significant increase in the consumption of oxygen (70 μM) compared to that in unactivated control cells and cells exposed to DPI prior to stimulation.

The process of phagocytosis in insect hemocytes is not fully understood, but plasmatocytes and hemocytes have been shown to have receptors similar to those of macrophages (27). Several studies carried out with bivalve hemocytes have shown the ability of these cells to phagocytose immediately after contact with a variety of nonself materials, including bacteria (48, 52) and yeast cells (49). Another study carried out with the same cell type demonstrated that phagocytosis is associated with lysosomal NADPH oxidase activity of membranes (71). In our study there was a remarkable similarity between the rates of phagocytosis of opsonized *C. albicans* by neutrophils and hemocytes (Fig. 1). Phagocytosis had a clear time-dependent index, and the percentages of cells that phagocytosed opsonized yeast cells in 60 min were comparable for the two immune cell types. Furthermore, significant reductions in superoxide production (Fig. 4) and microbial killing (Fig. 2) were observed when the hemocytes were incubated with DPI. These observations confirm the suggestion of previous workers (55) that phagocytosis of foreign materials by hemocytes stimulates the respiratory burst pathway involving NADPH oxidase activity and illustrate that superoxide production is necessary for efficient microbial killing by both neutrophils and hemocytes.

The functional similarities between hemocytes and phagocytic neutrophils prompted us to search for components of the NADPH oxidase of neutrophils in insect hemocytes. In a previous investigation, the presence of $p47^{phox}$ and $p67^{phox}$ in plant cells was examined (24), and the results indicated that there was a direct correlation between the presence of the two *phox* proteins and a quantitative oxidative burst. In our study an immunological approach was taken, in which we probed hemocyte cell lysates with polyclonal antibodies raised against the human forms of $gp91^{phox}$, $p40^{phox}$, $p47^{phox}$, and $p67^{phox}$.

In the immunoblots shown in Fig. 5 a strong broad band for $gp91^{phox}$ in insect hemocytes is visible, but it migrated on SDS gels at a lower molecular mass, approximately 70 kDa. There are three main subgroups of the NADPH oxidase families (NOXs), and the $gp91^{phox}$ subfamily consists of Nox1, $gp91^{phox}$, Nox3, and Nox4, all of which have molecular masses of approximately 65 kDa, a molecular mass similar to that of the immunoreactive protein of insect hemocytes. If this protein has a mechanism similar to that of $gp91^{phox}$, we would expect that it would transport electrons across membranes, with oxygen as the probable recipient, resulting in the formation of superoxide.

$p67^{phox}$ is a 59.7-kDa protein and is rich in motifs involved in protein-protein interactions (Fig. 8A). This protein is absolutely required to induce electron transport through flavocytochrome, and a defect in the gene is known to give rise to the autosomal form of CGD (33). As determined by Western blotting (Fig. 5C) and immunoprecipitation (Fig. 7), the antibodies raised against neutrophil $p67^{phox}$ reacted with a protein that was a similar size in the insect hemocyte lysates. MALDI-TOF analysis of this protein gave rise to a number of peptides, some of which fell within the two SH3 and PB1 domains of neutrophil $p67^{phox}$. The importance of these domains is apparent, as the C-terminal SH3 domain of $p67^{phox}$ is required for binding to the proline-rich motif of $p47^{phox}$ (28, 46) and $p67^{phox}$ binds to $p40^{phox}$ through the PB1 domain (50). Peptides of these binding motifs were found in the insect 67-kDa protein, and by analogy with $p67^{phox}$, it would be expected that this protein has the ability to interact with other proteins, although the main binding partner, $p40^{phox}$, was not detected in the insect cell lysate. The requirement for $p40^{phox}$ in the neutrophil NADPH oxidase remains obscure. Studies done in several different laboratories have suggested both negative (17) and positive regulatory roles (66) and, more recently, a role in the translocation of $p47^{phox}$ and $p67^{phox}$ to the vacuolar membrane upon activation (43).

Like $p67^{phox}$, $p47^{phox}$ is essential for functional NADPH oxidase activity and has previously been shown to be missing in most cases of autosomal recessive CGD (33). $p47^{phox}$ has a molecular mass of 44.6 kDa, and phosphorylation of this protein has been correlated with activation of the oxidase and occurs at the C-terminal end, in which 9 or 10 serine phosphorylation sites have been identified by phosphopeptide sequencing and site-directed mutagenesis (26). Several kinases are known to phosphorylate $p47^{phox}$ in vitro; among these kinases is protein kinase C, which was successfully identified in insect hemocytes lysate (Fig. 5G). The results of Western blotting (Fig. 5D) and immunoprecipitation analyses (Fig. 7) revealed the presence of a protein immunologically similar to $p47^{phox}$ of neutrophils in the hemocytes of *G. mellonella.* As determined by immunohistochemistry, the insect 47-kDa protein was found throughout the cytoplasm and the periphery of the cell (Fig. 6). This distribution of $p47^{phox}$ has previously been observed in unactivated neutrophils, and a possible regulatory role for $p47^{phox}$ in the reorganization of the cytoskeleton accompanying superoxide generation has been suggested (34). MALDI-TOF analysis of the insect 47-kDa protein gave rise to a number of peptides which covered 16% of neutrophil

p47^{phox} (Fig. 8C and D), including a portion of the p47^{phox} PX domain (involved in phosphoinositide binding).

The minimal requirement for in vitro cell-free oxidase activity has been recognized as lipid-reconstituted cytochrome (neutrophil membrane extract or recombinant), p47^{phox}, p67^{phox}, and rac (in the GTP-bound state) together with NADPH and anionic amphiphiles such as arachidonic acid or SDS (9). rac 2 is the predominant form in neutrophils and was also found in insect hemocytes (Fig. 5F). Therefore, in this study we identified immunologically related proteins (gp91^{phox}, p67^{phox}, p47^{phox}, and rac) for all the key proteins that are required in the cell-free oxidase system.

The findings presented in this paper illustrate the similarities at the cellular level between the human innate immune response and the insect immune response. Given the critical role of the innate immune response in protecting mammals from microbial infection and the high degree of structural and functional similarity between the mammalian and insect innate immune responses, studying the insect response to infection can provide data comparable to data which may be obtained using mammals (41). Larvae of *G. mellonella* have been used to evaluate the virulence of a range of bacteria and fungi, and more recently other insect species such as *D. melanogaster* have been used to evaluate the pathogenicity of *Aspergillus* species (6). This work supports the validity of using insects to obtain data comparable to the data obtained by using mammals for assessing the virulence of microbial pathogens.

ACKNOWLEDGMENTS

This work was supported by funding from the Higher Education Authority through PTRLI 3.

We gratefully acknowledge Alan Murphy for assistance with the MALDI-TOF MS analysis.

REFERENCES

1. **Arumugam, M., B. Romestand, J. Torreilles, and P. Roch.** 2000. *In vitro* production of superoxide and nitric oxide (as nitrite and nitrate) by *Mytilus galloprovincialis* haemocytes upon incubation with PMA or laminarin or during yeast phagocytosis. Eur. J. Cell Biol. **79:**513–519.
2. **Babior, B. M., R. S. Kipnes, and J. T. Curnutte.** 1973. Biological defence mechanisms: the production by leukocytes of superoxide, a potential bactericidal agent. J. Clin. Investig. **52:**741–744.
3. **Baggiolini, M., W. Ruch, and P. H. Cooper.** 1986. Measurement of hydrogen peroxide production by phagocytes using homovanillic acid and horse radish peroxidase. Methods Enzymol. **132:**395–400.
4. **Balls, M.** 1999. Science without guinea pigs. Res. Teach. Dev. Inf. **24:**26–28.
5. **Banfi, B., R. A. Clark, K. Steger, and K. H. Krause.** 2003. Two novel proteins activate superoxide generation by the NADPH oxidase NOX1. J. Biol. Chem. **278:**3510–3513.
6. **Bhabhra, R., M. D. Miley, E. Mylonakis, D. Boettner, J. Fortwendel, J. C. Panepinto, M. Postow, J. C. Rhodes, and D. S. Askew.** 2004. Disruption of the *Aspergillus fumigatus* gene encoding nucleolar protein CgrA impairs thermotolerant growth and reduces virulence. Infect. Immun. **72:**4731–4740.
7. **Boman, H. G., and D. Hultmark.** 1987. Cell-free immunity in insects. Annu. Rev. Microbiol. **41:**103–126.
8. **Brennan, M., D. Y. Thomas, M. Whiteway, and K. Kavanagh.** 2002. Correlation between virulence of *Candida albicans* mutants in mice and *Galleria mellonella* larvae. FEMS Immunol. Med. Micobiol. **34:**153–157.
9. **Bromberg, Y., and E. Pick.** 1984. Unsaturated fatty acids stimulate NADPH-dependent superoxide production by cell-free system derived from macrophages. Cell. Immunol. **88:**213–221.
10. **Cheng, G., Z. Cao, X. Xu, E. G. van Meir, and J. D. Lambeth.** 2001. Homologs of gp91^{phox}: cloning and tissue expression of Nox3, Nox4, and Nox5. Gene **269:**131–140.
11. **Cotter, G., S. Doyle, and K. Kavanagh.** 2000. Development of an insect model for the *in vivo* pathogenicity testing of yeasts. FEMS Immunol. Med. Micobiol. **27:**163–169.
12. **Cross, A. R., and O. T. Jones.** 1986. The effect of the inhibitor diphenylene iodonium on the superoxide-generating system of neutrophils. Specific labelling of a component polypeptide of the oxidase. Biochem. J. **237:**111–116.
13. **Curnutte, J. T., R. Kuver, and B. M. Babior.** 1987. Activation of the respiratory burst oxidase in a fully soluble system from human neutrophils. J. Biol. Chem. **262:**6450–6452.
14. **Dekker, L. V., M. Leitges, G. Altschuler, N. Mistry, A. McDermott, J. Roes, and A. W. Segal.** 2000. Protein kinase C-beta contributes to NADPH oxidase activation in neutrophils. Biochem. J. **347:**285–289.
15. **DeLeo, F. R., W. M. Nauseef, A. S. Jesaitis, J. Burritt, R. A. Clark, and M. T. Quinn.** 1995. A domain of p47^{phox} that interacts with human neutrophil flavocytochrome b558. J. Biol. Chem. **270:**26246–26251.
16. **DeLeo, F. R., K. V. Ulman, A. R. Davis, K. L. Jutila, and M. T. Quinn.** 1996. Assembly of the human neutrophil NADPH oxidase involves binding of p67^{phox} and flavocytochrome b to a common functional domain in p47^{phox}. J. Biol. Chem. **271:**17013–17020.
17. **de Mendez, I., and T. L. Leto.** 1995. Functional reconstitution of the phagocyte NADPH oxidase by transfection of its multiple components in a heterologous system. Blood **85:**1104–1110.
18. **Dewald, B., M. Thelen, and M. Baggiolini.** 1988. Two transduction sequences are necessary for neutrophil activation by receptor agonists. J. Biol. Chem. **263:**16179–16184.
19. **Diebold, B. A., and G. M. Bokoch.** 2001. Molecular basis for Rac2 regulation of phagocyte NADPH oxidase. Nat. Immunol. **2:**211–215.
20. **Diekmann, D., A. Abo, C. Johnston, A. W. Segal, and A. Hall.** 1994. Interaction of Rac with p67^{phox} and regulation of phagocytic NADPH oxidase activity. Science **265:**531–533.
21. **Dinauer, M. C., E. A. Pierce, R. W. Erickson, T. J. Muhlebach, H. Messner, S. H. Orkin, R. A. Seger, and J. T. Curnutte.** 1991. Point mutation in the cytoplasmic domain of the neutrophil p22^{phox} cytochrome b subunit is associated with a nonfunctional NADPH oxidase and chronic granulomatous disease. Proc. Natl. Acad. Sci. USA **88:**11231–11235.
22. **Dunphy, G., D. Morton, A. Kropinski, and J. Chadwick.** 1986. Pathogenicity of lipopolysaccharide mutants in *Pseudomonas aeruginosa* for larvae of *Galleria mellonella*: bacterial properties associated with virulence. J. Invertebr. Pathol. **47:**48–55.
23. **Dupuy, C., R. Ohayon, A. Valent, M. S. Noel-Hudson, D. Deme, and A. Virion.** 1999. Purification of a novel flavoprotein involved in the thyroid NADPH oxidase. Cloning of the porcine and human cDNAs. J. Biol. Chem. **274:**37265–37269.
24. **Dwyer, S. C., L. Legendre, P. S. Low, and T. L. Leto.** 1996. Plant and human neutrophil oxidative burst complexes contain immunologically related proteins. Biochim. Biophys. Acta **1289:**231–237.
25. **el Benna, J., L. P. Faust, and B. M. Babior.** 1994. The phosphorylation of the respiratory burst oxidase component p47^{phox} during neutrophil activation. Phosphorylation of sites recognized by protein kinase C and by proline-directed kinases. J. Biol. Chem. **269:**23431–23436.
26. **el Benna, J., L. P. Faust, J. L. Johnson, and B. M. Babior.** 1996. Phosphorylation of the respiratory burst oxidsae subunit p47^{phox} as determined by two-dimensional phosphopeptide mapping. Phosphorylation by protein kinase C, protein kinase A and a mitogen-activated protein kinase. J. Biol. Chem. **271:**6374–6378.
27. **Franc, N. C., J. L. Dimarca, M. Lagueux, J. Hoffmann, and R. A. Ezekowitz.** 1996. Croquemort, a novel *Drosophila* hemocyte/macrophage receptor that recognizes apoptotic cells. Immunity **4:**431–443.
28. **Fuchs, A., M. C. Dagher, J. Faure, and P. V. Vignais.** 1996. Topological organization of the cytosolic activating complex of the superoxide-generating NADPH oxidase. Pinpointing the sites of interaction between p47^{phox}, p67^{phox} and p40^{phox} using the two-hybrid system. Biochim. Biophys. Acta **1312:**39–47.
29. **Fuchs, A., M. C. Dagher, and P. V. Vignais.** 1995. Mapping the domains of interaction of p40^{phox} with both p47^{phox} and p67^{phox} of the neutrophil oxidase complex using the two-hybrid system. J. Biol. Chem. **270:**5695–5697.
30. **Geistz, M., J. B. Kopp, P. Varnai, and T. L. Leto.** 2000. Identification of renox, an NAD(P)H oxidase in kidney. Proc. Natl. Acad. Sci. USA **97:** 8010–8014.
31. **Geiszt, M., K. Lekstrom, J. Witta, and T. L. Leto.** 2003. Proteins homologous to p47^{phox} and p67^{phox} support superoxide production by NAD(P)H oxidase 1 in colon epithelial cells. J. Biol. Chem. **278:**20006–20012.
32. **Glupov, V. V., M. F. Khvoshevskaya, Y. L. Lovinskaya, I. M. Dubovski, V. V. Martemyanov, and J. Y. Sokolova.** 2001. Application of the nitroblue tetrazolium reduction method for studies on the production of reactive oxygen species in insect haemocytes. Cytobios **106:**165–178.
33. **Goldblatt, D., and A. J. Thrasher.** 2000. Chronic granulomatous disease. Clin. Exp. Immunol. **122:**1–9.
34. **Grogan, A., E. Reeves, N. Keep, F. Wientjes, N. F. Totty, A. L. Burlingame, J. J. Hsuan, and A. W. Segal.** 1997. Cytosolic phox proteins interact with and regulate the assembly of coronin in neutrophils. J. Cell Sci. **110:**3071–3081.
35. **Groom, Q. J., M. A. Torres, A. P. Fordham-Skelton, K. E. Hammond-Kosack, N. J. Robinson, and J. D. Jones.** 1996. *rbohA*, a rice homologue of the mammalian gp91^{phox} respiratory burst oxidase gene. Plant J. **10:**515–522.
36. **Hamamoto, H., K. Kurokawa, C. Kaito, K. Kamura, I. Manitra Razanajatovo, H. Kusuhara, T. Santa, and K. Sekimizu.** 2004. Quantitative evaluation of the therapeutic effects of antibiotics using silkworms infected with human pathogenic microorganisms. Antimicrob. Agents Chemother. **48:**774–779.

37. **Hampton, M. B., A. J. Kettle, and C. C. Winterbourn.** 1998. Inside the neutrophil phagosome: oxidants, myeloperoxidase, and bacterial killing. Blood **92:**3007–3017.
38. **Harper, A. M., M. F. Chaplin, and A. W. Segal.** 1985. Cytochrome b-245 from human neutrophils is a glycoprotein. Biochem. J. **227:**783–788.
39. **Henderson, L. M., and J. B. Chappell.** 1996. NADPH oxidase of neutrophils. Biochim. Biophys. Acta **1273:**87–107.
40. **Jander, G., L. G. Rahme, and F. M. Ausbel.** 2000. Positive correlation between virulence of *Pseudomonas aeruginosa* mutants in mice and insects. J. Bacteriol. **182:**3843–3845.
41. **Kavanagh, K., and E. P. Reeves.** 2004. Exploiting the potential of insects for the *in vivo* pathogenicity testing of microbial pathogens. FEMS Microbiol. Rev. **28:**101–112.
42. **Knaus, U. G., P. G. Heyworth, T. Evans, J. T. Curnutte, and G. M. Bokoch.** 1991. Regulation of phagocyte oxygen radical production by the GTP-binding protein Rac2. Science **254:**1512–1515.
43. **Kuribayashi, F., H. Nunoi, K. Wakamatsu, S. Tsunawaki, K. Sato, T. Ito, and H. Sumimoto.** 2002. The adaptor protein p40(phox) as a positive regulator of the superoxide-producing phagocyte oxidase. EMBO J. **21:**6312–6320.
44. **Laemmli, U. K.** 1970. Cleavage of structural proteins during the assembly of the head of bacteriophage T4. Nature **277:**680–685.
45. **Lamberth, J., G. Cheng, R. Arnold, and W. Edens.** 2000. Novel homologs of gp91phox. Trends Biochem. Sci. **25:**459–461.
46. **Leto, T. L., A. G. Adams, and I. de Mendez.** 1994. Assembly of the phagocyte NADPH oxidase: binding of Scr homology 3 domain to proline-rich targets. Proc. Natl. Acad. Sci. USA **91:**10650–10654.
47. **Medzhitov, R., P. Preston-Hulburt, and C. A. Janeway, Jr.** 1997. A human homologue of the *Drosophila* Toll protein signals activation of adaptive immunity. Nature **388:**394–397.
48. **Mortensen, S. H., and J. Glette.** 1996. Phagocytic activity of scallop (*Pecten maximus*) hemocytes maintained *in vitro*. Fish Shellfish Immunol. **6:**111–121.
49. **Mullainadhan, P., and L. Renwrantz.** 1986. Lectin-dependent recognition of foreign cells by hemocytes of the mussel, *Mytilus edulis*. Immunobiology **171:**263–273.
50. **Nakamura, R., M. Sumimoto, K. Mizuki, K. Hata, T. Ago, S. Kitajima, K. Takeshige, Y. Sakaki, and T. Ito.** 1998. The PC motif: a novel and evolutionarily conserved sequence involved in interactions between $p40^{phox}$ and $p67^{phox}$, SH3 domain-containing cytosolic factors of the phagocytic NADPH oxidase. Eur. J. Biochem. **251:**583–589.
51. **Nappi, A. J., and E. Vass.** 1998. Melanogenesis and the generation of cytotoxic molecules during insect cellular immune reactions. Pigment Cell Res. **6:**117–126.
52. **Oubella, R., P. Paillard, P. Maes, and M. Auffret.** 1994. Changes in hemolymph parameters in Manila clam *Ruditapes philippinarum* (Mollusca, Bivalvia) following bacterial challenge. J. Invertebr. Pathol. **64:**33–38.
53. **Ponting, C. P.** 1996. Novel domains in NADPH oxidase subunits, sorting nexins, and PtdIns 3-kinase: binding partners of SH3 domains? Protein Sci. **5:**2353–2357.
54. **Ratcliffe, N. A.** 1993. Cellular defence responses in insects: unresolved problems, p. 579–604. *In* N. E. Bechage, S. N. Thompson, and B. A. Federice (ed.), Parasites and pathogens of insects, vol. 1. Academic Press, San Diego, Calif.
55. **Reeves, E. P., H. Lu, J. Hugues Lortat, C. G. Messina, S. Bolsover, G. Gabella, E. O. Potma, A. Warley, J. Roes, and A. W. Segal.** 2002. Killing activity of neutrophils is mediated through activation of proteases by K^+ flux. Nature **416:**291–297.
56. **Reeves, E. P., C. G. Messina, S. Doyle, and K. Kavanagh.** 2004. Correlation between gliotoxin production and virulence of *Aspergillus fumigatus* in *Galleria mellonella*. Mycopathologia **158:**73–79.
57. **Salzet, M.** 2001. Vertebrate innate immunity resembles a mosaic of invertebrate immune responses. Trends Immunol. **22:**285–288.
58. **Segal, A. W., and O. T. Jones.** 1980. Rapid incorporation of the human neutrophil plasma membrane cytochrome b into phagocytic vacuoles. Biochem. Biophys. Res. Commun. **92:**710–715.
59. **Segal, A. W., and O. T. G. Jones.** 1978. Novel cytochrome b system in phagocytic vacuoles of human granulocytes. Nature **276:**515–517.
60. **Segal, A. W., and S. B. Coade.** 1978. Kinetics of oxygen consumption by phagocytosing human neutrophils. Biochem. Biophys. Res. Commun. **84:**611–617.
61. **Segal, A. W., I. West, F. Wientjes, J. H. Nugent, A. J. Chavan, B. Haley, R. C. Garcia, H. Rosen, and G. Scrace.** 1992. Cytochrome b-245 is a flavocytochrome containing FAD and the NADPH-binding site of the microbicidal oxidase of phagocytes. Biochem. J. **284:**781–788.
62. **Slepneva, I. A., V. V. Glupov, S. V. Sergeeva, and V. V. Khramtsov.** 1999. EPR detection of reactive oxygen species in hemolymph of *Galleria mellonella* and *Dendrolimus superans sibiricus* (Lepidoptera) larvae. Biochem. Biophys. Res. Commun. **264:**212–215.
63. **Soderhall, K., and L. Cerenius.** 1998. Role of the prophenoloxidase activating system in invertebrate immunity. Curr. Opin. Immunol. **10:**23–28.
64. **Sumimoto, H., K. Hata, K. Mizuki, T. Ito, Y. Kaga, Y. Sakaki, Y. Fukumaki, M. Nakamura, and K. Takeshige.** 1996. Assembly and activation of the phagocyte NADPH oxidase. Specific interaction of the N-terminal Src homology 3 domain of p47phox with p22phox is required for activation of the NADPH oxidase. J. Biol. Chem. **271:**22152–22158.
65. **Tojo, S., F. Naganuma, K. Arakawa, and S. Yokool.** 2000. Involvement of both granular cells and plasmatocytes in phagocytic reactions in the greater wax moth, *Galleria mellonella*. J. Insect Physiol. **46:**1129–1135.
66. **Tsunawaki, S., S. Kagara, K. Yoshikawa, L. S. Yoshida, T. Kuratsuji, and H. Namiki.** 1996. Involvement of $p40^{phox}$ in activation of phagocyte NADPH oxidase through association of its carboxyl-terminal, but not its amino-terminal, with $p67^{phox}$. J. Exp. Med. **184:**893–902.
67. **Vilmos, P., and E. Kurucz.** 1998. Insect immunity: evolutionary roots of the mammalian innate immune system. Immunol. Lett. **62:**59–66.
68. **Wallach, T. M., and A. W. Segal.** 1996. Stoichiometry of the subunits of flavocytochrome b558 of the NADPH oxidase of phagocytes. Biochem. J. **320:**33–38.
69. **Wientjes, F. B., J. J. Hsuan, N. F. Totty, and A. W. Segal.** 1993. $p40^{phox}$, a third cytosolic component of the activation complex of the NADPH oxidase to contain Src homology 3 domains. Biochem. J. **296:**557–561.
70. **Wientjes, F. B., G. Panayotou, E. Reeves, and A. W. Segal.** 1996. Interactions between cytosolic components of the NADPH oxidase: $p40^{phox}$ interacts with both $p67^{phox}$ and $p47^{phox}$. Biochem. J. **317:**919–924.
71. **Winston, G. W., M. N. Moore, M. A. Kirchin, and C. Soverchia.** 1996. Production of reactive oxygen species by haemocytes from the marine mussel *Mytilus edulis*: lysosomal localization and effect of xenobiotics. Comp. Biochem. Physiol. Part C **113:**221–229.
72. **Wymann, M. P., V. von Tscharner, D. A. Deranleau, and M. Baggiolini.** 1987. Chemiluminescence detection of H_2O_2 produced by human neutrophils during the respiratory burst. Anal. Biochem. **165:**371–378.

Editor: T. R. Kozel